Journal of Stress Analysis
Vol. 9, No. 1, 2025, 81-93
Bu-Ali Sina University

ORIGINAL RESEARCH PAPER

Finite Element Analysis of CAREM-25 Modular Reactor Pressure Vessel Using ASME-Sec8-Div2-Part5 Code

Mojtaba Zolfaghari[a,*], **Mahdi Astaraki**[b], **Hamed Heydari**[c]

[a] Department of Mechanical Engineering, Arak University, Iran.
[b] Department of Mechanical Engineering, Technical and Engineering Faculty, Arak University, Arak, Iran.
[c] School of Mechanic Engineering, Shahrekord University, Shahrekord, Iran.

Article info

Article history:
Received 12 August 2024
Received in revised form
01 June 2025
Accepted 15 June 2025

Keywords:
Reactor pressure vessel
Pressure vessels
ASME code
CAREM25
ABAQUS
SMR

Abstract

This paper deals with the simulation of the pressure vessel of a small modular reactor, which is one of the most key components of nuclear power plants. In this regard, based on the two main factors of pressure and temperature and considering the operating realities, various load combinations were extracted based on ASME Sec. VIII Div. 2 Part 5, and finite element analysis was performed based on the ASME algorithm for reactor pressure vessel analysis and using standard failure modes, as well as other design considerations. Also, effective factors in the design and safety of the vessel were considered, and finally, by giving the required inputs to the Abaqus finite element software, the software outputs were analyzed. The results obtained indicate that the mechanical design based on ASME-Sec8-Div2-Part5 is largely consistent with the results of the design based on the nuclear section (ASME-Sec3). Because the results had almost the same thickness as the CAREM-25 small modular reactor vessel. Finally, it can be concluded that using the ASME standard along with finite element software and modern finite element-assisted solution methods largely meets the needs of the pressure vessel design department in small modular nuclear power plants.

1. Introduction

Nuclear energy is a critical clean energy source for reducing environmental pollutants, and small modular reactors (SMRs) have emerged as a promising solution to meet the increasing global energy demand. Among SMRs, the CAREM-25, a pressurized light water reactor, represents a significant advancement due to its compact design and potential for deployment in diverse settings. The reactor pressure vessel, a key component, must withstand extreme conditions, including high pressure (12.25MPa), high temperature (326°C), and challenges such as radiation brittleness, thermal stresses, fatigue, corrosion, and creep [1, 2]. Ensuring the structural integrity of the pressure vessel is essential for the safety and efficiency of SMRs, necessitating advanced design and analysis methods.

Argentina's CAREM reactor is one of the world's first integrated small modular pressurized light water reactors, which was designed by the National Atomic Energy Comission of Argentina and some affiliated nuclear companies. The CAREM reactor has an electric power of 25MW (though some reports also cite 27MW) and a thermal power of 100MW [4].

Fig. 1. shows a view of the pressurized vessel of the CAREM-25 reactor.

It should be mentioned that the CAREM-25 reactor is primarily designed for prototyping and testing

*Corresponding author: M. Zolfaghari (Assistant Professor)
E-mail address: m-zolfaghari@araku.ac.ir
10.22084/jrstan.2025.28156.1247
ISSN: 2588-2597

various components, so that in case of success, such reactors with an output power of 150 to 300 megawatts of electricity will be produced [6]. The pressure vessel of the CAREM-25 reactor has a height of 11 meters, a diameter of 3.2 meters, and a variable thickness of 13cm to 20cm. The reactor vessel is made of forged steel with internal cladding of stainless steel. Table 1 shows the design parameters of the CAREM-25 reactor.

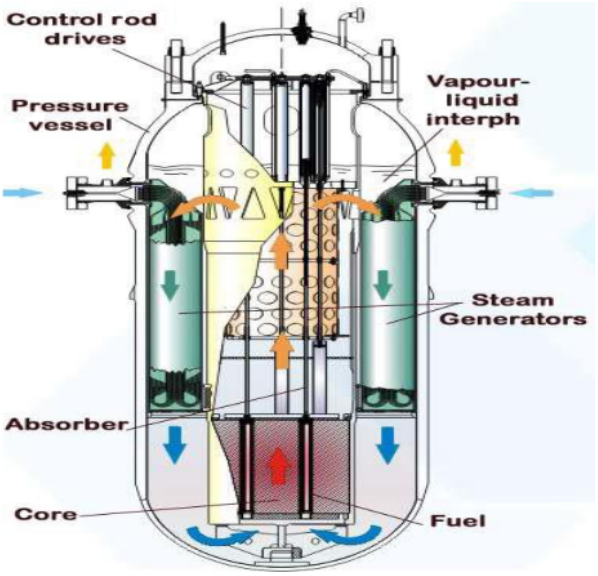

Fig. 1. A view of the CAREM-25 pressurized vessel [5].

Research and development in the field of modular reactors with small dimensions and high safety has been one of the most important topics of scientific research in the last decade, as they have been developed and are continuing to be developed in some countries, including: the United States, Canada, France, Russia, China, Japan, South Korea, Argentina, Brazil, South Africa, and India, and conceptual and operational plans for this type of reactors have been presented [7]. Notable features of modular reactors include a simple design, high intrinsic safety, higher efficiency and effectiveness, lower operating cost, increased service life and long-term performance, no need for fuel for several years, and the multiple use for the production of fresh water was pointed out. Also, due to the small dimensions of this type of reactors and their construction as a single unit, it is possible to easily carry and install them in remote areas or in small towns. The studies conducted in the field of small modular reactors are not extensive; therefore, some of them are as follows: In 2014, Zitav and Cooper reviewed the technology and design of modular reactors and compared the characteristics of different types of these reactors. Also, safety issues and economic considerations of modular reactors were researched. Their studies show that modular reactors have more superiority and safety compared to other reactors [8,9]. In addition, in 2014, Ingersoll et al. investigated NuScale modular reactors, and their studies show that NuScale power plants have the ability to be coupled with hybrid power plants and power plants that are capable of desalination and would be very economical [10]. Kim et al. presented papers in the fourth international conference on small and medium-sized reactors as new options for nuclear power plants in countries, examining the design development and review of modular pressurized water reactors [11]. In an article, Aghababaei and Nedai examined the reactor pressure vessel and evaluated the stresses caused by thermal shocks during a periodic thermal transient using Abaqus software.

Table 1
Reactor parameters CAREM-25 [2].

Parameter	Description
Technology developer, country of origin	CNEA, Argentina
Reactor type	Integral PWR
Coolant/moderator	Light water / Light water
Thermal/electrical capacity, MW(t)/MW(e)	100/ 30
Primary circulation	Natural circulation
NSSS Operating Pressure (primary/secondary), MPa	12.25/ 4.7
Core Inlet/Outlet CoolantTemperature ($\mathcal{C}^{\wedge\circ}$)	284/ 326
Fuel type/assembly array	UO2 pellet/hexagonal
Fuel enrichment (%)	3.1% (prototype)
Core Discharge Burnup (GWd/ton)	24 (prototype)
Refueling Cycle (months)	14 (prototype)
Reactivity control mechanism	Control rod driving
Approach to safety systems	Passive
Design life (years)	40
RPV height/diameter (m)	11 / 3.2
Seismic Design (SSE)	0.25g
Fuel Cycle Requirements	390 full-power days and 50%
or Approach	of core replacement (prototype)

Their studies showed that the middle areas of the core and the welding area are the most critical areas in terms of stress concentration due to the presence of stress concentrations [3]. Alexenko et al. studied the basic factors governing the influence of neutron radiation on the mechanical properties of steel used in the pressurized vessel of a reactor [12]. Also, Honarkar et al. conducted a computational analysis of the safety margin for crack growth in the pressure vessel of a reactor. Their results showed that the high flow of neutrons on the areas around the reactor core led to an increase in the brittleness of the materials of the pressure vessel and a decrease in the safety margin for crack growth under accident conditions on the inner surface of the reactor chamber [13].

In 2015, Gawande conducted a study aimed at confirming the structural strength of the pressure vessel cover instead of the expensive hydrostatic test with an analytical approach in accordance with the ASME-Sec8-Div2 [14]. Also in 2000, in a report, Ishida addressed the process of developing new nuclear power plants, including the CAREM project [15]. Although several published reports have mentioned various technical aspects of the CAREM modular reactor, the pressure vessel of this reactor has been mentioned less in articles and reports. In this research, the finite elements of the pressure vessel of the CAREM-25 modular reactor were investigated. In 2016, Vishal et al. in an article analyzed the steam boiler drum under high pressure and temperature. The results showed that the design based on the five parts of the ASME code will have a significant effect on reducing the thickness and economic efficiency [16]. In 2019, Kabani et al. in a study evaluated and validated pressure equipment using the ASME-Sec8-Div2 [17]. Mirsky et al. studied pressure vessels and steam boilers using Sec8-Div2 [18]. In 2010, Sims et al, conducted a study on pressure vessels in the marine industry. Their results showed that the use of Sec8-Div2 resulted in better material utilization and better productivity than Div1 [19]. Zandi and Kamerkhani conducted research in the field of analysis of internal pressure vessel using ANSYS finite element software. The analysis of the results has shown the criticality of the area near the fillet where the vertical column wall of the vessel is connected to its head [20]. Chan et al, conducted an experimental study to better determine the failure mechanism of the pressure vessel on foundations. They concluded that the failure mechanism is influenced by two factors, first, the ratio of the thickness to the radius of the pressure vessel, and second, the type of tank foundation [21].

This study aims to evaluate the structural integrity of the CAREM-25 reactor pressure vessel using finite element analysis (FEA) based on ASME Section VIII, Division 2, Part 5, and to validate its applicability against nuclear-specific standards (ASME Section III). By employing Abaqus software, we analyze the vessel under realistic operating conditions, considering multiple failure modes—overall failure, local failure, buckling, and ratcheting—through elastic, elastic-plastic, and limit load methods. The objective is to demonstrate that this approach meets the safety and design needs of SMR pressure vessels, providing practical insights for nuclear engineering applications

2. Materials and Methods

Geometrical modeling of CAREM-25 pressure vessel and finite element analysis was performed using ABAQUS software. Considering that the vessel is symmetrical in terms of geometry and boundary conditions, in order to simplify and reduce the computation time, one-quarter of the vessel was modeled, and loads, boundary conditions and meshing were applied on this part. The properties of the imported material correspond to SA508-Grade3-Class1 steel. These properties are obtained according to ASME-Sec2-PartD at temperatures from 25 to 326°C. Also, the ultimate stress value was 552MPa, the density was $7.75\times10^{-9}(\frac{ton}{mm^3})$ and the Poisson's ratio was 0.3 at a temperature of 326 degrees Celsius. And finally, the allowable stress of the material used, based on load factors, construction methods, and design type, was found to be 192MPa.

Table 2
Properties extracted from ASME-Sec 2-Part D at different working temperatures [22].

T (C°)	E (GPa)	TE[1] $(\frac{10^{-6}}{℃})$	TC[2] $(\frac{w}{m.℃})$	SH $(\frac{10^6.mj}{ton.℃})$	s_y (MPa)
25	191	11.5	41	445.68	345
100	187	12.1	40.6	481.49	323
150	184	12.4	40.4	504.63	314
200	181	12.7	40.1	526.9	305
250	178	13	39.5	546.86	299
300	174	13.3	38.7	566.16	292
326	172.5	13.4	38.3	576.65	289

1. Thermal Expansion
2. Thermal Conductivity

The analyzed problem was performed in the mechanical and thermal coupling section, which is defined in the STEP module for the problem. The temperatures of the inner and outer walls of the container were set to 326 and 20 degrees Celsius, respectively. Here the maximum internal pressure for the vessel was defined as 12.25MPa.

Meshing was carried out in the Mesh module The best available mesh type and elements were selected. Displacement-temperature coupled elements were used for the problem, , with a hexahedral (Hex) element shape and a structured meshing technique including C3D20RT elements. Also, the meshing of the vessel is shown in Fig. 2.

A mesh sensitivity analysis was conducted for the pressurized vessel to ensure the optimal mesh size to

increase the convergence and accuracy of the numerical results. The maximum equivalent plastic strain (PEEQ) occurring in the structure was used as the convergence criterion, the results of which are shown in Fig. 3. The number of members ranged from 2000 to 14000. In this case, it was observed that the meshes provided sufficient sensitivity for the vessel under pressure.

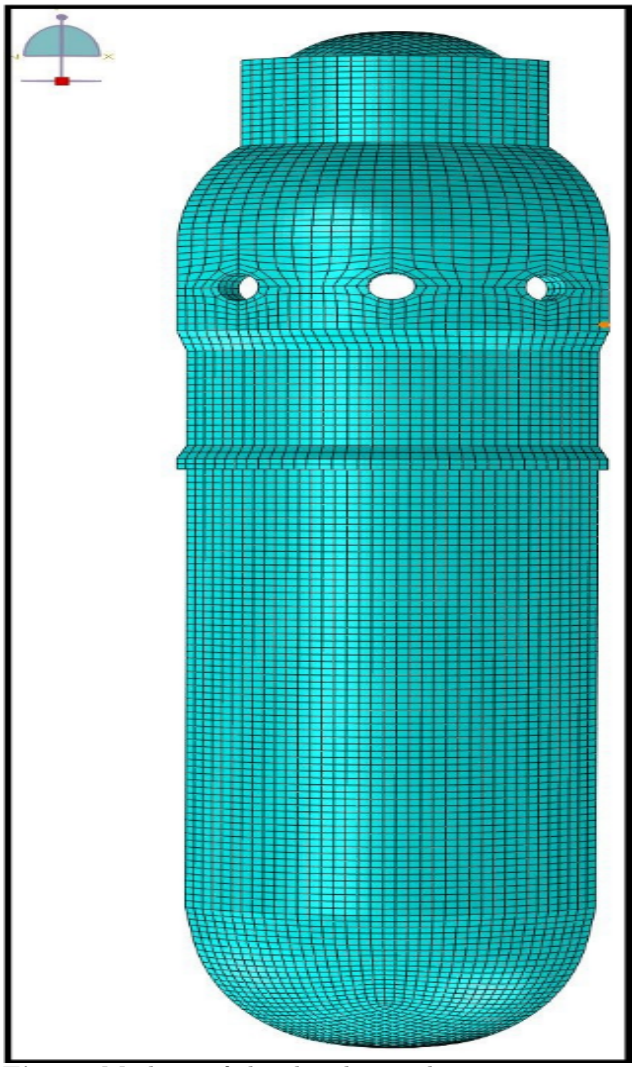

Fig. 2. Meshing of the chamber under pressure.

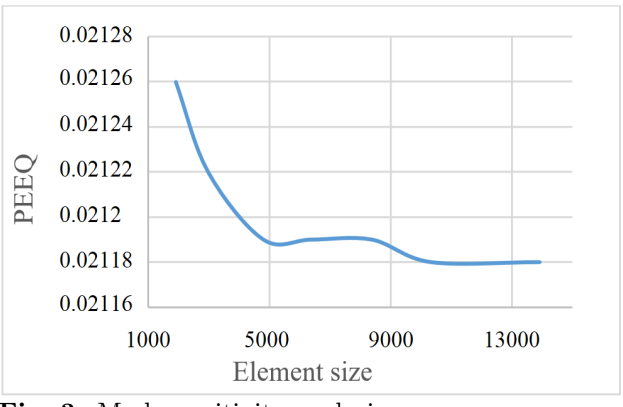

Fig. 3. Mesh sensitivity analysis.

3. Results and Discussion

3.1. Evaluation of Overall Failure of the Vessel Under Pressure by Elastic Method

To determine the acceptability of a device, the equivalent stresses calculated must be lower than the allowable stress. Figure 5.1 of the ASME-Sec8-Div2-Part5 code shows a schematic of the classification of equivalent stresses and corresponding allowable stresses.The forces considered in the design, as specified in Table 5.1 ('Load Descriptions') of ASME Section VIII, Division 2, Part 5 [23], include internal pressure (12.25MPa), thermal loads (326°C inner wall, 20°C outer wall), and other mechanical loads. Additional combinations may also be considered if necessary, based on specific requirements and past experience Also, the combination of loading conditions and allowable loads for elastic analysis is shown in Table 5.1 in the code [23].

After performing the elastic analysis by choosing the suitable plane and linearization lines, the stress linearization in the examined path is conducted. Finite element software directly extracts membrane, bending and maximum stresses using linearization capability. After classifying the stresses using Table 5.6. from the code, it is determined whether the membrane stresses are P_L or P_m, as well as P_b or the secondary bending stresses. It should be noted that the secondary and peak stresses in the overall failure do not need to be considered in the elastic method. Secondary and peak stresses are used to evaluate fatigue and strain cycle growth using the elastic method. Linearization should be done according to Von Mises criterion.

To evaluate the elastic failure, the calculated equivalent stress value should be compared with its allowable values as follows.

$$P_m = S \quad , \quad P_L = S_{PL} \quad , \quad P_L + P_b \leq S_{PL}$$

where S is the allowable stress value of the material at the design temperature and S_{PL} is the highest value of the following numbers:

a) 1.5 times the allowable stress value of the material at the design temperature

b) The yield stress of the material (S_y), except for the conditions where the ratio of the yield stress of the material to its ultimate stress is greater than 0.7 or when the properties of the material are time-dependent, the value (a) should be used as S_{PL}.

The model is analyzed using Abaqus software. Fig. 4. shows the equivalent stress distribution in the model. This stress is actually the sum of membrane stress, bending stress and peak stress.

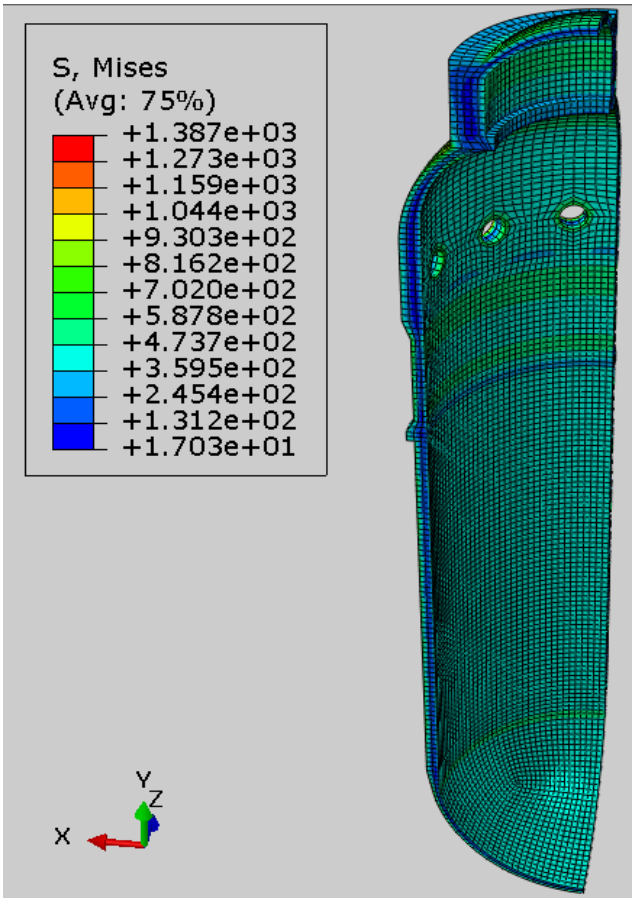

Fig. 4. Equivalent stress distribution on the model.

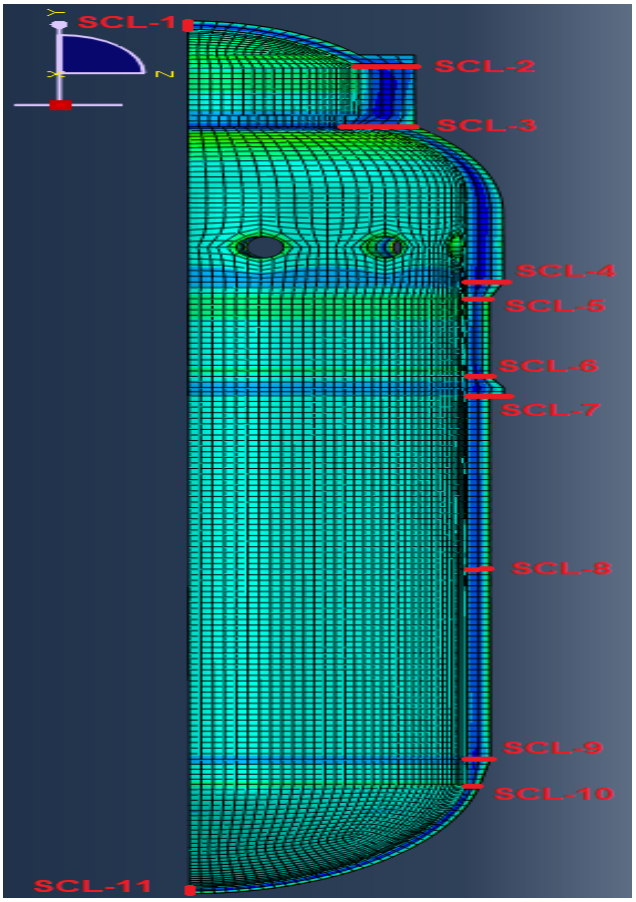

Fig. 5. Linearization lines (SCL) in the model.

To separate the stresses and calculate the membrane stresses, it is necessary to define the stress linearization lines. linear stresses are calculated by defining the path in the software. In general, the choice of the path should be defined by the location of two points along the thickness. Therefore, linearization lines in the model are created according to Fig. 5.

Stresses are categorized. Secondary and peak stresses need not be considered in plastic failure analysis. the stresses obtained from the results of linearization are categorized according to Table 3, and then the stresses P_m.P_L.P_b are compared with their allowable values.

Table 3
Elastic analysis result.

SCL No.			Div.2- 2019			Equivalent Linearized Stresses (MPa)			Stress Evaluation	Stress Evaluation	
	Location	Material	S (MPa)	S_y (MPa)	SPL (MPa) [max(1.5S,Sy)]	Pm	PL	Pb	Pm<S	PL<SPL	PL+Pb<SPL
1	Dished head crown	SA508-Gr3-Cl1	192	289	289	80.4	N/A	518.42	pass	N/A	**Not pass**
2	Head to shelltransition	SA508-Gr3-Cl1	192	289	289	N/A	71.92	N/A	N/A	pass	pass
3	Head to shelltransition	SA508-Gr3-Cl1	192	289	289	N/A	20.39	N/A	N/A	pass	pass
4	Shell (awayfromdiscontinuities)	SA508-Gr3-Cl1	192	289	289	123.46	N/A	N/A	pass	N/A	N/A
5	Shell (discontinuities)	SA508-Gr3-Cl1	192	289	289	N/A	143.66	N/A	N/A	Pass	Pass
6	Shell (discontinuities)	SA508-Gr3-Cl1	192	289	289	N/A	82.64	N/A	N/A	Pass	Pass
7	Shell (discontinuities)	SA508-Gr3-Cl1	192	289	289	N/A	194.64	N/A	N/A	Pass	Pass
8	Shell (awayfromdiscontinuities)	SA508-Gr3-Cl1	192	289	289	140.17	N/A	N/A	Pass	N/A	N/A
9	Head to shelltransition	SA508-Gr3-Cl1	192	289	289	N/A	116.94	N/A	N/A	pass	N/A
10	Head tangentline	SA508-Gr3-Cl1	192	289	289	N/A	202	N/A	N/A	pass	pass
11	Dished head crown	SA508-Gr3-Cl1	192	289	289	144.87	N/A	537.86	Pass	N/A	**Not pass**

3.2. Limit Load Method

Calculations are performed to obtain the lower limit of the component loading value. The permissible load value is obtained by applying a coefficient on the load limit so that the vessel does not enter the plastic regime. This method is one of the alternative methods to evaluate vessels and its components to prevent overall failure, which can be used instead of the elastic method and linearization to meet primary stress requirements mentioned in the elastic method. The displacements and strains obtained in this method have no physical significance. If there is a limit on any of the above variables, the elastic-plastic method should be applied.

The incoming loads are applied. the internal pressure should be multiplied by a factor of 1.5.

$$1.5 \times 12.25\text{MPa} = 18.375\text{MPa}$$

The fully plastic elastic material model is applied considering the small displacement theory.

The yield stress is equal to:

$$1.5 \times S = 1.5 \times 192 = 288\text{MPa}$$

The analysis is performed. In case of convergence, the components are immune to plastic failure.

Here, the desired analysis is convergent for the limit load method (Fig. 6.) and therefore the components are acceptable for total failure according to the above method.

To obtain the limit load of the chamber under pressure, the loading amount must be selected such that it exceeds the actual limit load. As a result, at a certain time, the software cannot continue the analysis and convergence does not occur, and the balance equation is no longer established. This defines the limit load. Here, the internal pressure applied in the analysis is considered 40MPa.

The last converged solution in the software occurs at time=0.761. And since time-proportional loading is applied, the final load value is as follows:

$$0.761 \times 40\text{MPa} = 30.44\text{MPa}$$

According to reference [20], when using the limit force, the design factor of 1.5 on the internal pressure must be considered. As a result, the maximum (limit) pressure is equal to:

$$\frac{30.44}{1.5} = 20.29\text{MPa}$$

3.3. Elastic-Plastic Method

In this method, the breaking load of the vessel is obtained by considering the input forces and the characteristics of deformation of the components using elastic-plastic analysis. The allowable load value is obtained by applying a design factor to the plastic collapse load. The elastic-plastic method is a more accurate method than the elastic and limit load methods because the real behavior of the geometry is estimated more accurately. The stress redistribution due to the plastic deformation of the equipment (strain hardening effect) and the deformation characteristics of the material are directly included in the analysis. At first, we should obtain the actual stress-strain curve by using the relationships related to Sec8 Div2 Annex-3D and use the obtained information as input in Abaqus software. Fig. 7 shows the actual stress-strain curve for SA508-Gr3-Cl1 material.

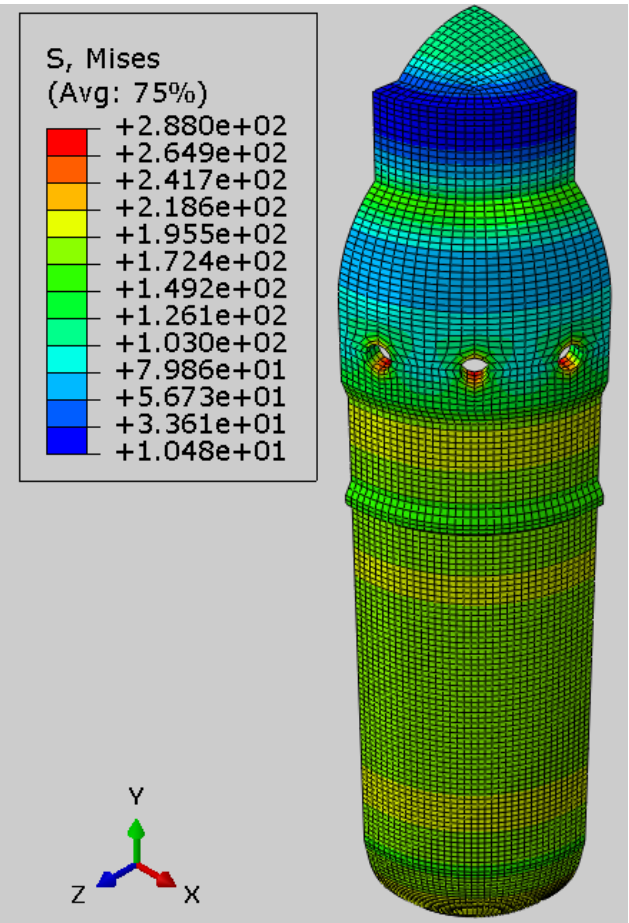

Fig. 6. Results related to limit load method.

3.3.1. Evaluation of the Overall Failure of the Studied Vessel by Elastic-Plastic Method

The incoming loads are applied. The internal pressure must be multiplied by a factor of 2.4.

$$2.4 \times 12.25 = 29.4\text{MPa}$$

The real stress-strain curve data of the material is applied, and the vessel is analyzed using the large displacement theory as shown in Table 4.

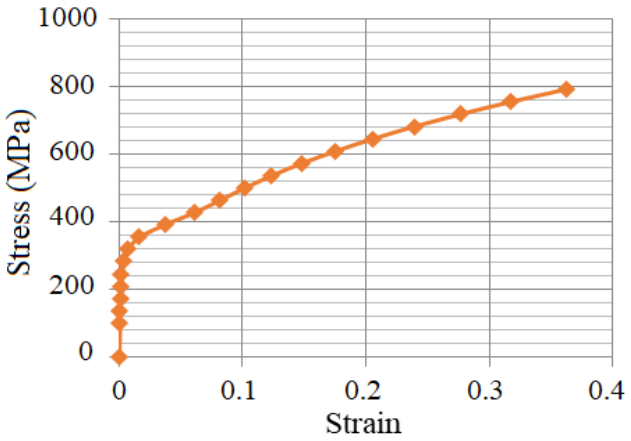

Fig. 7. Actual stress-strain curve of SA508 Gr3 CL1 at 326°C.

Table 4
Actual stress-strain curve data of SA508 Gr3 Cl-1.

s_t(MPa)	e_t	Plastic strain
100.00	0.000581	0.00000
136.27	0.0008	0.00022
172.54	0.001052	0.00047
208.80	0.001412	0.00083
245.07	0.00207	0.00149
281.34	0.0035	0.00292
317.61	0.007062	0.00648
353.88	0.016683	0.01610
390.14	0.037179	0.03660
426.41	0.061343	0.06076
462.68	0.081959	0.08138
498.95	0.101933	0.10135
535.22	0.123746	0.12317
571.49	0.148216	0.14763
607.75	0.175622	0.17504
644.02	0.206124	0.20554
680.29	0.239863	0.23928
716.56	0.27698	0.27640
752.83	0.317616	0.31704
789.09	0.361912	0.36133

The load factor and the boundary conditions are applied and the analysis is perfromed. If the analysis is carried out to the end and the solution converges, this means that the loading is below the failure threshold of the component. Otherwise, it is necessary to revise the component design of the part. Here the problem converged. Therefore, the above components are stable against overall failure according to the elastic-plastic analysis, and since the nonlinear analysis was carried out through the entire loading process, the intended loading is within the acceptable range. Fig. 8 shows the equivalent stress distribution on the model.

3.4. Protection Against Local Failure

In addition to the protection of pressure vessels against overall failure, local failure criteria must also be evaluated for their components. If the examined component is designed based on Div2, Part 4, the above failure model does not need to be checked.

Two methods, elastic and elastic-plastic, can be used to evaluate local failure. Both of the following methods can be used to evaluate local failure when the overall failure is evaluated using the limit load method and found to be acceptable.

a) Elastic method - gives an estimate of local failure according to elastic analysis.

b) The elastic-plastic method is a more accurate method for evaluating local failure according to the elastic-plastic analysis.

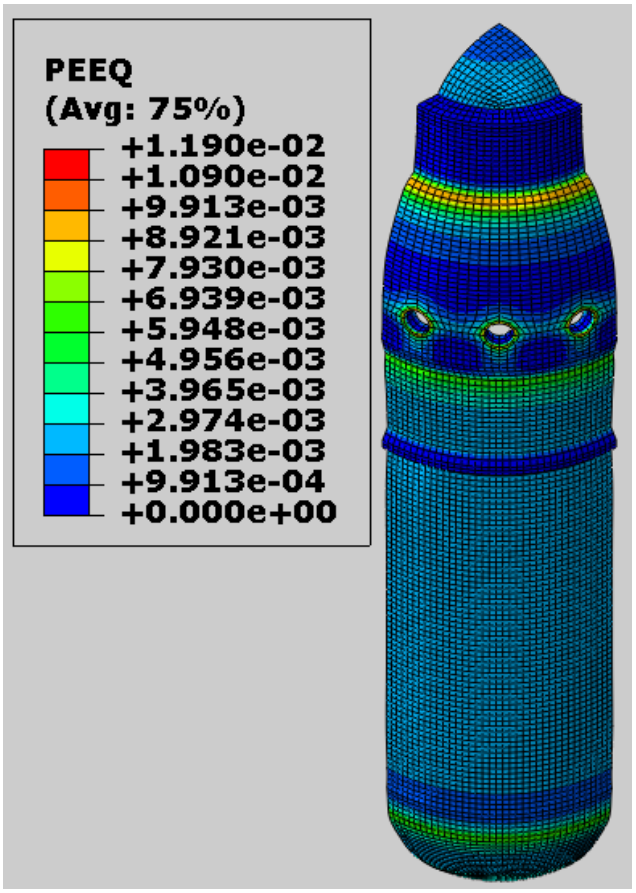

Fig. 8. Equivalent stress distribution on the model.

3.4.1. Assessment of Local Failure Using the Elastic Method

At first, the algebraic sum of the main linearized stresses in the examined points must be according to

the following criteria:

$$(s_1+s_2+s_3) \leq 4S$$

This means that to check the local failure, the algebraic sum of the main linearized stresses must be less than or equal to four times the allowable stress at the design temperature.

As you can see in Fig. 9, the obtained values (using the relation $\left|\frac{s_1+s_2+s_3}{4S}\right| \leq 1$) are greater than one, which indicates that the results in the elastic method are unacceptable.

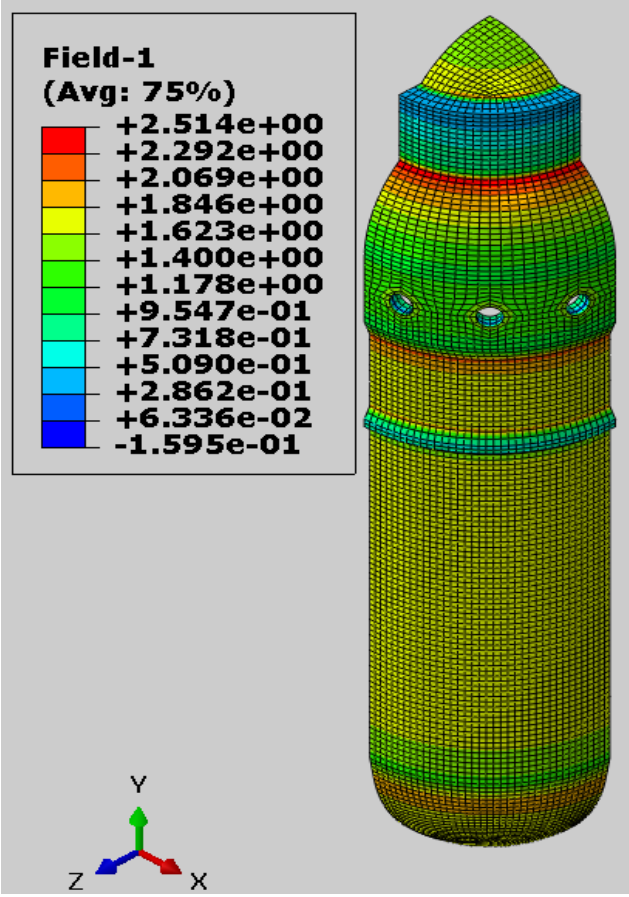

Fig. 9. The results of elastic analysis in local failure assessment.

3.4.2. Evaluation of Local Failure of Pressure Vessel Using Elastic-Plastic Method

Based on the content mentioned in the code, we multiply the internal pressure by a factor of 1.7. Non-linear geometry effect must be enabled.

$$1.7 \times 12.25 = 20.825\text{MPa}$$

For each point that is examined, we obtain the value of the main stresses (s_1, s_2 and s_3), the equivalent stress (s_e) and the equivalent plastic strain (e_{peq}).

We obtain the triaxial strain range (e_L) using Eq. (1) (we obtain the constants a_{sl}, m_2 and e_{Lu} from table (5-7) in the code).

$$1e_L{=}e_{Lu} \times \exp[-\left(\frac{a_{sl}}{1+m_2}\right)\left(\left\{\frac{(s_1+s_2+s_3)}{3s_e}\right\}-\frac{1}{3}\right) \quad (1)$$

If Relation (2) is established for the examined points in the relevant loading combination, the design is acceptable.

$$e_{peq}+e_{cf} \leq e_L \quad (2)$$

The forming strain value is considered to be zero since it is assumed that heat treatment has been performed on the vessel

$$e_{cf}=0$$

Fig. 10 illustrates the equivalent plastic strain contour. To evaluate all components, the ratio ($\frac{e_{eq}+e_{cf}}{e_L}$) is shown in Fig. 11. As you can see, this ratio is below one in all points, indicating that the components are resistant to local failure.

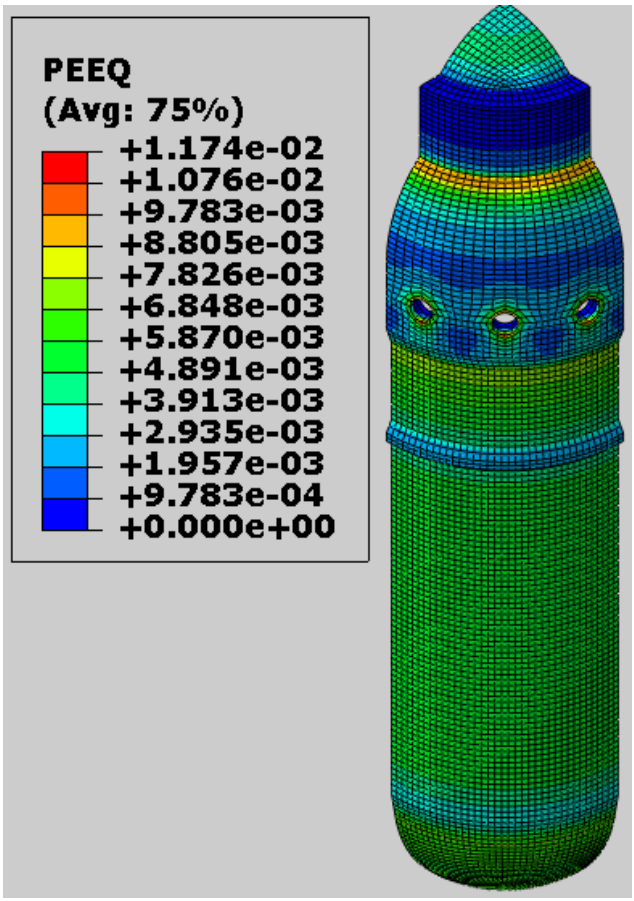

Fig. 10. Equivalent plastic strain contour.

3.5. Buckling

In addition to protection against total failure of pressure vessels, if there is a compressive stress field in the vessel as a result of the applied loading combination, a safety factor must also be considered to protect the equipment against buckling.

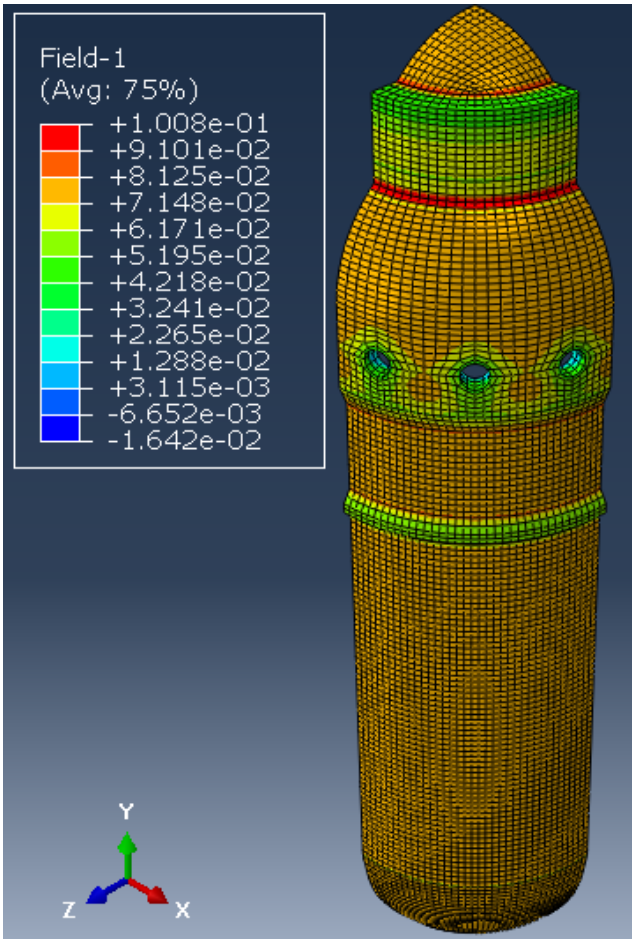

Fig. 11. Contour of ratio $(\frac{e_{eq}+e_{cf}}{e_L})$.

3.5.1. Buckling Evaluation of the Studied Vessel Under External Pressure

Here, the vessel under study is investigated under external pressure. The purpose of this analysis is to calculate the buckling load and compare it with the allowable buckling load.

For linear (elastic) buckling analysis, the value of the design factor is equal to $\emptyset_B = \frac{2}{\beta_{cr}}$. Also, the value of β_{cr}= 0.8 has been used for the vessel. Therefore, the minimum confidence factor is obtained as follows:

$$\emptyset_B = \frac{2}{0.8} = 2.5$$

Considering that the buckling is sensitive to deformation, first the deformation of the vessel should be calculated, then the buckling analysis should be done. For this purpose, we created the linear buckling analysis and applied the results of the static analysis as pre-stress to the buckling analysis.

The allowable buckling load or the maximum allowable vacuum pressure are calculated using the following equation [24].

$$\text{Buckling Load} = \frac{(\text{Dead Loads}) + \text{Eigenvalues} \times (\text{Live Loads})}{\text{Design Factor}} \quad (3)$$

In this regard, we have:
Dead Loads=Total Load (Preload) before buckling step
Live Loads=Incremental (perturbation) Load in buckling step

The obtained results, as shown in Fig. 12, show the first eigenvalue is 362.45. Therefore, the allowable buckling load is as follows:

$$\text{Buckling Load} = \frac{(-0.1) + 362.45 \times (-0.1)}{2.5} = -14.53\text{MPa}$$

Since the maximum allowable external pressure (14.53MPa) is higher than the applied external pressure (0.1MPa), the vessel will not buckle. Also, in Fig. 13 Shows the results of the Static General analysis, which is applied as a pre-stress to the buckling analysis.

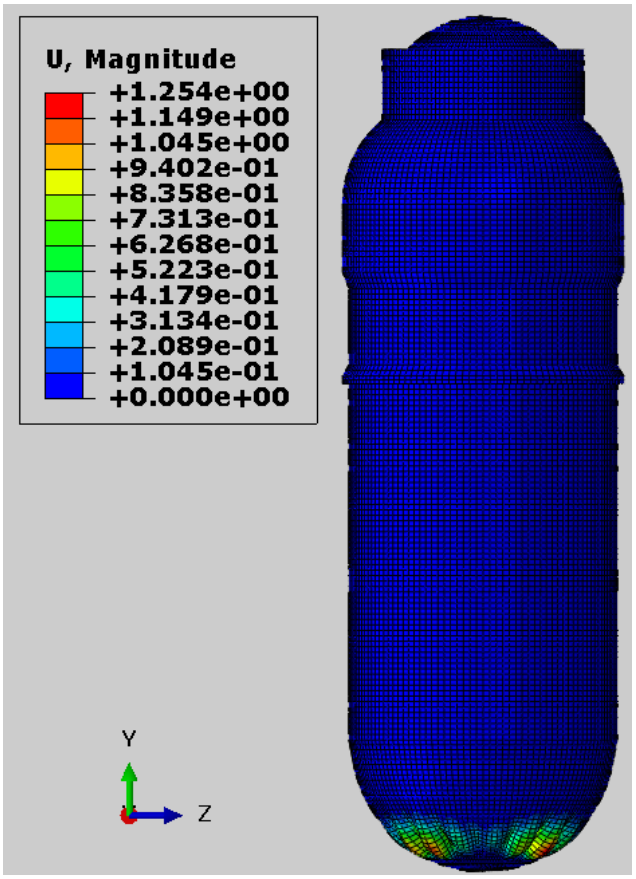

Fig. 12. Buckling analysis results using the elastic method.

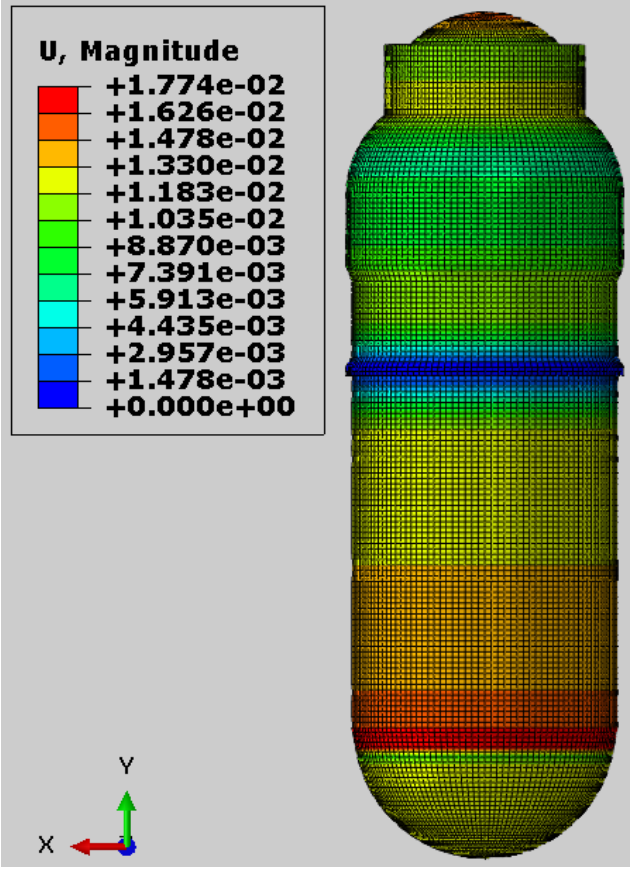

Fig. 13. General static analysis results.

Buckling analysis results considering nonlinear behavior.

3.5.2. Nonlinear Analysis of Buckling

For non-linear analysis, we use the Riks method. This method cannot predict buckling modes; thus, we have to enter the results of linear buckling analysis as input in this analysis. Here, the reliability coefficient is considered 2.4 according to Table (5-5) in reference [23]. And then we input the outputs of the buckling step as geometric imperfections in the Riks model. For this purpose, the results of the first method are considered, then we the software is instructed to save these results in the ODB file by adding the following code in the Edit Keywords section.

*Output, field, variable-PRESELECT
*node output
u,
*node file,global=yes
u,
*End Step

Then, in the Riks analysis, using the following code, we enter geometric imperfections from the previous step as input.
*End Part
**
*imperfection, file= File Name, step=2
1, 0.000015
3, 0.0000015
** ASSEMBLY

This method demonstrates the plastic failure analysis using the elastic-plastic method and the modeling of any type of deformation that may lead to vessel buckling, which is more accurate than the previous method. It should be noted that in this method, the capacity reduction factor is not used because unnecessary deformation is considered in the model. Fig. 14 exhibits the graph related to the results of this analysis where the vertical axis corresponds to the load factor and the horizontal axis corresponds to the displacement. According to the obtained results, the allowable buckling load value is 9.29, which is acceptable for the equipment.

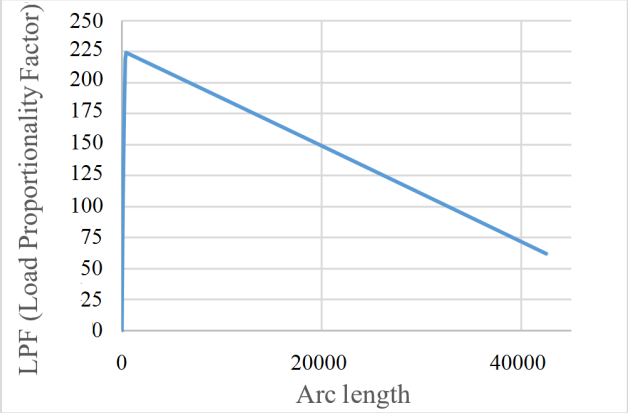

Fig. 14. Buckling behavior of the studied vessel using Riks analysis.

3.6. Protection Against Ratcheting

Deformation or plastic strain that increases in pressure vessel components due to cyclic stresses resulting from control load forces (pressure changes and external force) or control strain (temperature changes or applied displacement) leads to ratcheting in containers. Ratcheting leads to a change in the strain of the material, which causes failure due to fatigue, and at the same time, the plastic development strain of the system causes the failure of the equipment.

3.6.1. Ratcheting Evaluation of Pressurized Vessel by Elastic Method

First, the elastic analysis is performed according to section 5.1 of the article, and the stresses are linearized along the paths shown in Fig. 5. Then, the stresses are classified into $P_b.P_L.P_m$ and Q.

The interval set of primary and secondary stresses $\Delta S_{n.k}$ in each of the linearization lines are compared with its permissible values S_{ps} (Table 5).

Table 5
Ratcheting results by elastic method.

SCL No.	Location	Material	Div.2- 2019 S (MPa)	S_y (MPa)	S_{PS} (MPa) [max(3S,2Sy)]	$\Delta S_{n,k}$ P_L+P_b+Q	Stress valuation $\Delta S_{n,k} \leq S_{PS}$
1	Dished Head Crown	SA508-Gr3-Cl1	211	317	634	598.82	Pass
2	Head to shelltransition	SA508-Gr3-Cl1	211	317	634	344.23	Pass
3	Head to shelltransition	SA508-Gr3-Cl1	211	317	634	367.02	Pass
4	Shell (away fromdiscontinuities)	SA508-Gr3-Cl1	211	317	634	516.12	Pass
5	Shell (discontinuities)	SA508-Gr3-Cl1	211	317	634	737.17	**Not Pass**
6	Shell (discontinuities)	SA508-Gr3-Cl1	211	317	634	603.9	Pass
7	Shell (discontinuities)	SA508-Gr3-Cl1	211	317	634	589.62	Pass
8	Shell (away fromdiscontinuities)	SA508-Gr3-Cl1	211	317	634	659.86	**Not Pass**
9	Head to shelltransition	SA508-Gr3-Cl1	211	317	634	558.6	Pass
10	Head tangent Line	SA508-Gr3-Cl1	211	317	634	834.87	**Not Pass**
11	Dished Head Crown	SA508-Gr3-Cl1	211	317	634	682.74	**Not Pass**

It should be noted that $S_u.S_y$ *and* S depend on the type of part. Also, the value of S_{ps} is a function of S_y and S which are a function of temperature. In order to obtain S_y and S in a cycle, one must first find the minimum and maximum temperatures in the cycle, and then calculate the values of S_y and S for these two temperatures. The average values in these two temperatures represent the final values of S_y and S, which are used in the calculation of S_{ps}. This means that the value of S_{ps} can be different in each cycle. Therefore, the allowable and yield stress are obtained at the minimum and maximum temperatures of the cycle. (The range of applied stress here is from zero pressure to working pressure. Since there is no stress at zero pressure, the total range of primary and secondary stresses is equal to its value at working pressure.) The following shows how S_{ps} is obtained.

$$\begin{cases} T = 326℃ & \rightarrow S = 192\text{Mpa} \\ T = 20℃ & \rightarrow S = 230\text{Mpa} \end{cases}$$

$$\text{Average} = 211\text{Mpa} \rightarrow S = 3 \times 211 = 633\text{Mpa}$$

$$\begin{cases} T = 326℃ & \rightarrow S_y = 289\text{Mpa} \\ T = 20℃ & \rightarrow S_y = 345\text{Mpa} \end{cases}$$

$$\text{Average} = 317\text{Mpa} \rightarrow S_y = 2 \times 317 = 634\text{Mpa}$$

$$S_{ps} = Max(3S.2S_y) = 634\text{Mpa}$$

According to the results of the elastic analysis in Table 4, ratcheting evaluation using the elastic method is not acceptable for the vessel under pressure.

3.6.2. Ratcheting Evaluation of Pressure Vessel by Elastic-Plastic Method

Based on the code requirements, the loading and unloading cycle is repeated at least three times; therefore, the applied loads are created in three steps in the Step module and then an Amplitude in the Load module. Subsequently, the settings and boundary conditions are applied. Figure 15 displays the results of plastic strain at the end of the third cycle. According to Figure 16, which is the curve of plastic strain corresponding to loading, the plastic strain value has remained constant since time one, indicating shakedown of the structure [23]. Therefore, ratcheting analysis using the elastic-plastic method for the vessel under pressure has acceptable results.

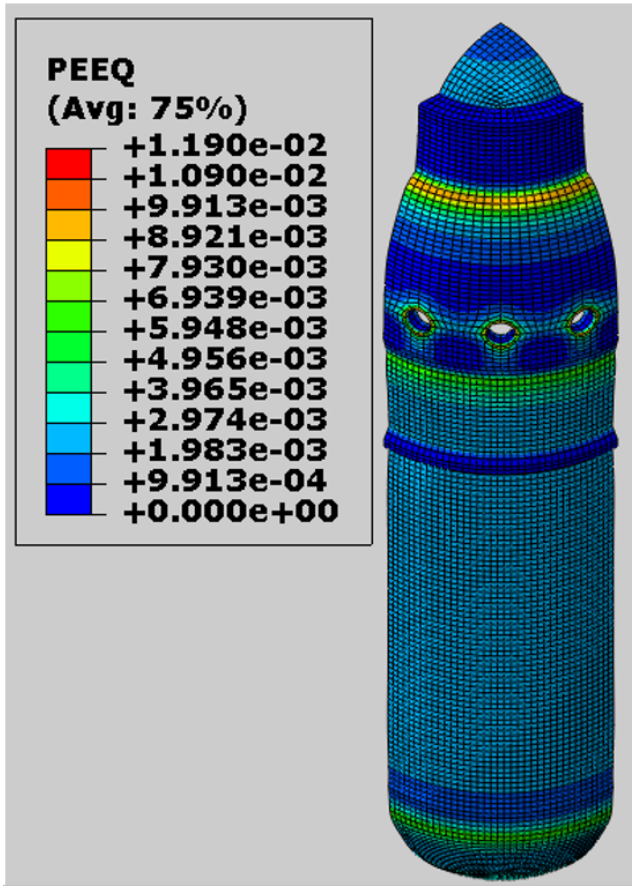

Fig. 15. The results of plastic strain at the end of the third cycle.

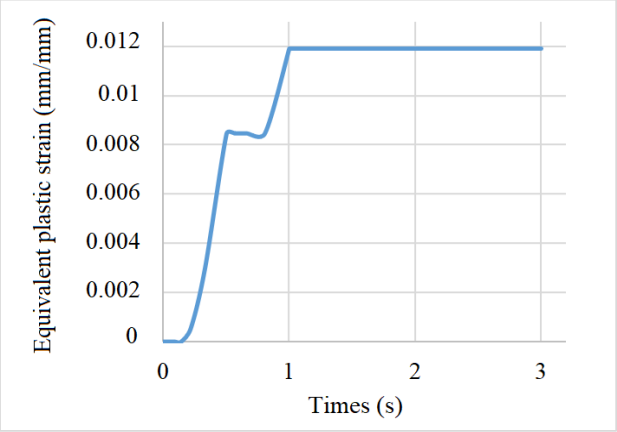

Fig. 16. Stability of plastic strain at the maximum point.

3.7. Validation

3.7.1. Comparison of Pressure Vessel Thickness Based on ASME-Sec8-Div2-Part4 and ASME-Sec3-Div1-NB

Following the mentioned contents related to Sec8-Div2, it should be noted that this division is further categorized into two parts of Class 1 and Class 2 based on the confidence factor used. The confidence factor of Class 1 is 3 and Class 2 is 2.4. To design based on the rules in Div2, reference should be made to the fourth part, which is based on Tresca's yield criterion. In this section, Eq. (4) is employed to obtain the thickness of the cylindrical part of the vessel, which is mentioned in paragraph 4.3.3.1 of the code, and Eq. (5) for the spherical part based on paragraph 4.3.5.1.

$$t = \frac{D}{2}\left(exp\left[\frac{P}{SE}\right] - 1\right) \tag{4}$$

$$t = \frac{D}{2}\left(exp\left[\frac{0.5P}{SE}\right] - 1\right) \tag{5}$$

In these equations, P=12.25MPa, E=1, S=184MPa and R=1590mm.

To obtain the allowable stress value (S) at a temperature of 326°C, we refer to ASME Section II, Part D, Table 2A, under the title Design Stress Intensity Values, Sm, for Ferrous Materials. This value can be used for designs in Section III, Division 1, Class 1 and Section VIII, Division 2, Class 1. At this temperature, the allowable stress (Sm) is 184MPa. Therefore, based on the corresponding equations, the required thicknesses for the cylindrical and spherical parts of the vessel are determined.

$$T_{Cyl} = \frac{3180}{2}\left(\exp\left[\frac{12.25}{184}\right] - 1\right) = 109.45\text{mm}$$

$$T_{Sph} = \frac{3180}{2}\left(\exp\left[\frac{0.5 \times 12.25}{184}\right] - 1\right) = 53.81\text{mm}$$

It is worth noting that the allowable stress value for use in Part 5 is given in Sec2-Part D-Table 5A under the title Maximum Allowable Stress Values, S, for Ferrous, and its value is 192MPa.

To obtain the thickness based on Sec3 Div1 NB-Class1, Eq. (6) given in paragraph 3324.1 of the code for the cylindrical part and also paragraph 3324.2 given for the spherical part is used according to Eq. (7).

$$T_{Cyl} = \frac{PR}{S_m - 0.5P} = \frac{12.25 \times 1590}{184 - (0.5 \times 12.25)} = 109.5\text{mm} \tag{6}$$

$$T_{Sph} = \frac{PR}{2S_m - P} = \frac{12.25 \times 1590}{(2 \times 184) - 12.25} = 54.75\text{mm} \tag{7}$$

By comparing the obtained results, a slight difference of the values in both parts of the code is noticeable. This slight difference, which is based on the design method based on analysis, is related to the greater thickness in Section 3 [25]. For validation, these values are controlled with the acceptable values obtained in this chapter based on Sec8-Div2-Part5, confirming the correctness of the results.

4. Conclusion

In this article, the simulation of the pressure vessel of a small modular reactor-one of the key components of nuclear power plants-is presented. First, the characteristics of pressure vessels are examined, followed by a discussion of the general design rules. Based on the two main factors of pressure and temperature, and considering actual operating conditions, various load cases were extracted, and finite element analysis was conducted using standard failure modes. The results showed that in the elastic method—which is considered conservative-some failure modes were not satisfied. However, all failure modes were satisfied using the elastic-plastic method, which provides greater accuracy and is one of the reasons for the optimal design outcome. In addition, the successful evaluation of buckling and ratcheting modes demonstrated the structure's capability to withstand combined loading conditions. Finally, based on the overall analysis, the vessel thickness showed a 16% increase compared to values obtained from analytical formulas.

References

[1] M. Chen, F. Lu, R. Wang, A. Ren, Structural integrity assessment of the reactor pressure vessel under the pressurized thermal shock loading, Nucl. Eng. Des., 272 (2014) 84-91.

[2] D. F. Mora, M. Niffenegger, G. Qian, M. Jaros, B. Niceno, Modelling of reactor pressure vessel

subjected to pressurized thermal shock using 3D-XFEM, Nucl. Eng. Des., 353 (2019) 110237.

[3] N. Amir, A. Farzin, Modeling of PWR reactor pressure chamber and evaluation of stresses caused by thermal shocks during a periodic period of thermal transients., in The first competition of the comprehensive international conference of engineering sciences in Iran, (2017).

[4] Z. G. Saeed, K. Nima, Small Modular Reactors in Nuclear Industry, Tehran: Simaye Danesh, (2021).

[5] A. International Atomic Energy, Advances in Small Modular Reactor Technology Developments A Supplement to: IAEA Advanced Reactors Information System (ARIS) 2020 Edition, International Atomic Energy Agency (IAEA), (2020).

[6] H. Shirani, Nuclear power plants and small modular reactors (SMRs), Construction Science and Techniques, 1(4) (2021) 35-51.

[7] E. S. Zarifi, F. Kamran Ghaffari, Neutronic Parameters Analyses of SMART Advanced Small Modular Reactor Core, in Iranian Physics Conference Paper, (2018).

[8] Z. Liu, J. Fan, Technology readiness assessment of Small Modular Reactor (SMR) designs, Prog. Nucl. Energy., 70 (2014) 20-28.

[9] M. Cooper, Small modular reactors and the future of nuclear power in the United States, Energy Res. Soc. Sci., 3 (2014) 161-177.

[10] D. T. Ingersoll, Z. J. Houghton, R. Bromm, C. Desportes, NuScale small modular reactor for Cogeneration of electricity and water, Desalination, 340 (2014) 84-93.

[11] S.-H. Kim, K. K. Kim, J. W. Yeo, M. H. Chang, S. Q. Zee, Design verification program of SMART, Technology, 1(2) (2003).

[12] N. N. Alekseenko, A. Amaev, I. Gorynin, V. Nikolaev, Radiation damage of nuclear power plant pressure vessel steels, (1997).

[13] M. R. Honarkar, K. Vaezi, A. Naeim Matajie Kajvari, R. Nazari, Simulating the failure mechanism of the pressure chamber of Bushehr reactor, in Iran nuclear conference, (2014).

[14] P. P. Devang Desai, Sangram A. Gawande, A Study on Design by Analysis Approach Accordance to Asme Code, 9, (2014).

[15] M. Ishida, Development of new nuclear power plant in Argentina.

[16] V. Payghan, D. N. Jadhav, G. Y. Savant, S. Bharadwaj, Design & Analysis of Steam Drum Based on ASME Boiler and Pressure Vessel Code, Section VIII Div. 2 & Div. 3. 511-517.

[17] A. El-Kabbany, Y. Miao, ASME Section VIII Div. 2 Finite Element Elastic Plastic Analysis MethodA Case Study.

[18] Z. Mirski, K. Banyś, Z. Faek, T. Piwowarczyk, FEM-aided Design of Welded Pressure Vessels According to ASME BPVC Regulations, Biuletyn Instytutu Spawalnictwa w Gliwicach, 58(5) (2014) 114-121.

[19] J. R. Sims, Engineered Pressure Vessels for Marine Service Using Asme Section VIII, Division 2 and Division 3 Pressure Vessel Codes.

[20] A. Zandi Baghcheh Maryam, S. Kamarkhani, Investigation and analysis of internal pressure vessels using ANSYS finite element software, in The second international conference on new research achievements in mechanics, industries and aerospace, (2017).

[21] G. Chan, A. Tooth, J. Spence, An experimental study of the collapse of horizontal saddle-supported storage vessels, Proceedings of the Institution of Mechanical Engineers, Proc. Inst. Mech. Eng. E, 212(3) (1998) 183-195.

[22] BPVC Section II-Materials-Part D-Properties, ASME, (2019) 1256.

[23] BPVC Section VIII-Rules for Construction of Pressure Vessels Division 2-Alternative Rules, ASME, (2019) 872.

[24] M. Torabi, Finite element design of pressure vessels and heat exchangers (according to ASME Sec. vlll Div. 2 - part 5): Idehnegar, (2019).

[25] D. L. P. E. DE experimentos, M. D. R. RA, Proyecto Integrador Carrera de Ingeniera Nuclear, (2014).